# SPECTRAL ANALYSIS AND GRAVITY MODELLING OF THE ALMAZÁN BASIN (CENTRAL SPAIN)*

C. Rey Moral [1,2], D. Gómez Ortiz [1,2] and R. Tejero [2]

[1] *Instituto Tecnológico Geominero de España (I.T.G.E.), Ríos Rosas 23, 28003 Madrid, Spain (E-mail: reymoral@eucmos.sim.ucm.es)*
[2] *Departamento de Geodinámica, Fac. CC. Geológicas, UCM, Ciudad Universitaria, 28040 Madrid, Spain*

* ***Trabajo presentado en el 11th Meeting of the Association of European Geological Societies (MAEGS-11, Alicante, 1999)***

**Abstract:** A study concerning the deep structure of the Almazán basin has been carried out by using seismic, gravity and geological data. A new interpretation of previous seismic reflection lines has provided an isopach map for the top Albian unit showing an overall simple flat-bottomed syncline geometry with a 4500 m thickness depocenter placed near the northeastern boundary of the basin. A gravity survey provided a gravity map of the basin and surrounding areas, depicting relative gravity highs and lows linked to sedimentary infill variations and lithological changes in the basement. A map for the theoretical gravity due to the sedimentary infill has been done by integrating the data derived from the isopach map with the function which describes the density increasing with depth. Substracting this map to the observed gravity map, a new one depicting the gravity response for the basement has been obtained. Spectral analysis of this new map shows the occurrence of a regional source located at 11 km. Integrating all the aforementioned data, three 2+1/2 D gravity models have been obtained. These models display an acceptable fitting linking surface geological structure with bottom basin geometry, as well as different basement bodies and the geometry of the boundary between the basement and middle crust.

**Key words:** Almazán basin, gravity, seismic reflection profiles, spectral analysis, modelling.

**Resumen:** La Cuenca de Almazán constituye una de las áreas subsidentes rellenas por sedimentos terciarios continentales, originadas durante la convergencia entre las placas europea y africana que tuvo lugar en la orogenia alpina (Armenteros *et al.*, 1989; Bond, 1996). Se ha obtenido el mapa de anomalías de Bouguer de la cuenca y áreas adyacentes, en el que aparece un mínimo gravimétrico de orientación NO-SE, bordeado por dos máximos que corresponden a las ramas aragonesa y castellana de la Cordillera Ibérica. Se ha obtenido un mapa de isopacas para el techo del Albiense a partir de una nueva interpretación de perfiles sísmicos de reflexión previos. La geometría general es la de un sinclinal de base plana con un depocentro de 4500 m de espesor situado cerca del extremo NE de la cuenca. La realización de una campaña gravimétrica ha permitido obtener un mapa de Anomalías de Bouguer de la cuenca y áreas adyacentes, mostrando máximos y mínimos gravimétricos relativos relacionados con variaciones del relleno sedimentario y cambios litológicos en el basamento. Integrando los datos obtenidos del mapa de isopacas con una función cuadrática que describe la variación de densidad en profundidad, se ha calculado el efecto gravimétrico teórico debido al relleno sedimentario. Restando este efecto al mapa de Anomalías de Bouguer observado, se ha obtenido un nuevo mapa que refleja la respuesta gravimétrica del basamento. Mediante el análisis espectral de este nuevo mapa ha podido determinarse la existencia de una fuente regional situada a 11 km de profundidad. Integrando todos los datos antes mencionados, se han obtenido tres modelos gravimétricos en 2+1/2 D. Estos modelos presentan un ajuste aceptable relacionando la estructura geológica superficial con la geometría del fondo de la cuenca, y muestran, diferentes cuerpos en el basamento y la geometría del límite entre corteza media y basamento.

**Palabras clave:** Cuenca de Almazán, perfiles sísmicos de reflexión, gravimetría, análisis espectral, modelización.

Rey Moral, C., Gómez Ortiz, D. & Tejero, R. (2000): Spectral analysis and Gravity Modelling of the Almazán Basin (Central Spain). *Rev. Soc. Geol. España,* 13 (1): 131-142

The inner part of the Iberian Plate was strongly deformed during the Tertiary due to the collision between Africa, Europe and Iberia, forming intra-plate mountain chains and continental basins (Sanz de Galdeano, 1996). The Iberian Range was one of those chains and the Almazán Basin is located within the Iberian Range

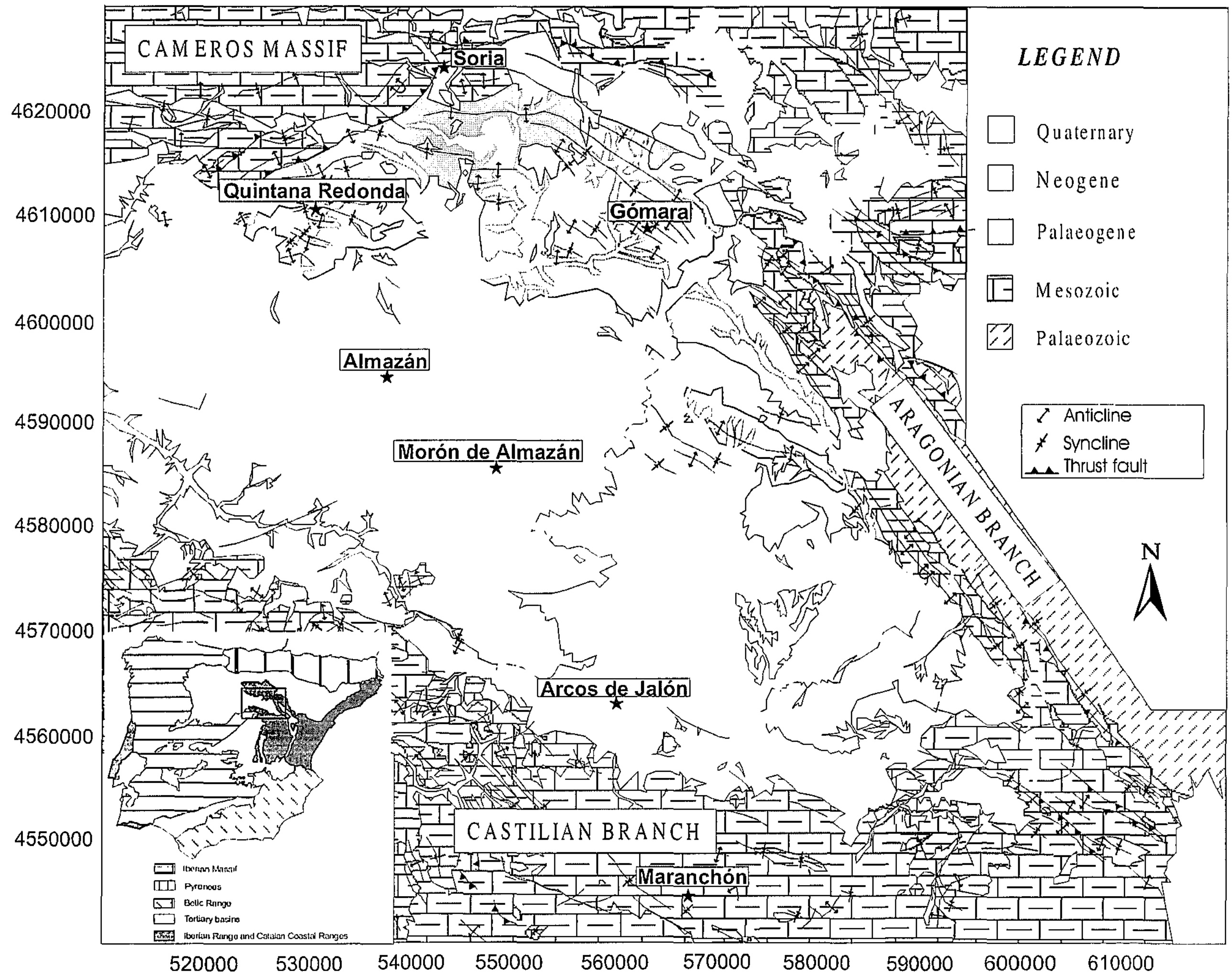


**Figure 1.-** Geological map of the Almazán Basin and location of the Almazán Basin within the Iberian peninsula. UTM coordinates in km. Huse 30.

at the easternmost part of the Duero Basin.

The basin was filled by Palaeogene and Neogene sediments, composed of alluvial deposits, with conglomerates and sandstones, near the basin borders, and shales, lacustrine limestones and gypsum towards the basin centre. The Palaeogene deposits (up to 3500 m in thickness) are folded and only crop out at the northeastern margin, whereas the Neogene formations (up to 500 m in thickness) remain horizontal onlapping the Mesozoic rocks of the southern border.

The basin is located between mountain ranges where older rocks (Palaeozoic and Mesozoic) crop out: the Aragonian branch of the Iberian Chain to the east, the Cameros massif and the Castillian branch of the Iberian Chain to the south (Fig. 1). The Aragonian branch of the Iberian Chain consists of a NW-SE trending antiform of Palaeozoic rocks (an up to 7000 m thick succession of sandstones and shales), bounded by Mesozoic sediments.

The Cameros Massif, resulting from the Tertiary inversion of the Mesozoic Cameros Basin, bounds the basin to the north with E-W trending faults, throwing up to 2-3 km to the south (Platt, 1990; Clemente and Pérez Arlucea, 1993; Guimerà *et al.*, 1995). It consists of Mesozoic rocks, mainly evaporites, sandstones and marine and lacustrine limestones, spanning Upper Jurassic to Lower Cretaceous times.

The Castillian branch of the Iberian Chain mainly consists of Triassic and Jurassic formations reaching a maximum thickness of 2000 m. The Triassic appears in Germanic facies: Buntsandstein (sandstones and shales), Muschelkalk (limestones, marls and evaporites) and Keuper (lutites and evaporites). The Jurassic formations consist mainly of marine limestones (Goy *et al.*, 1976; Goy and Suárez Vega, 1983). The top of the Mesozoic series is constituted by Albian sandstones and Upper Cretaceous limestones (García Hidalgo *et al.*, 1997). Main folds and faults in the area show a NNO-SSE to NNE-SSW trend.

The Almazán structure shows an overall simple flat-bottomed, syncline geometry. The maximum thickness of the preserved Tertiary deposits is located along an E-W trough that crosses the central part of the basin (ITGE, 1990; Bond, 1996; Casas *et al.* (in press)).

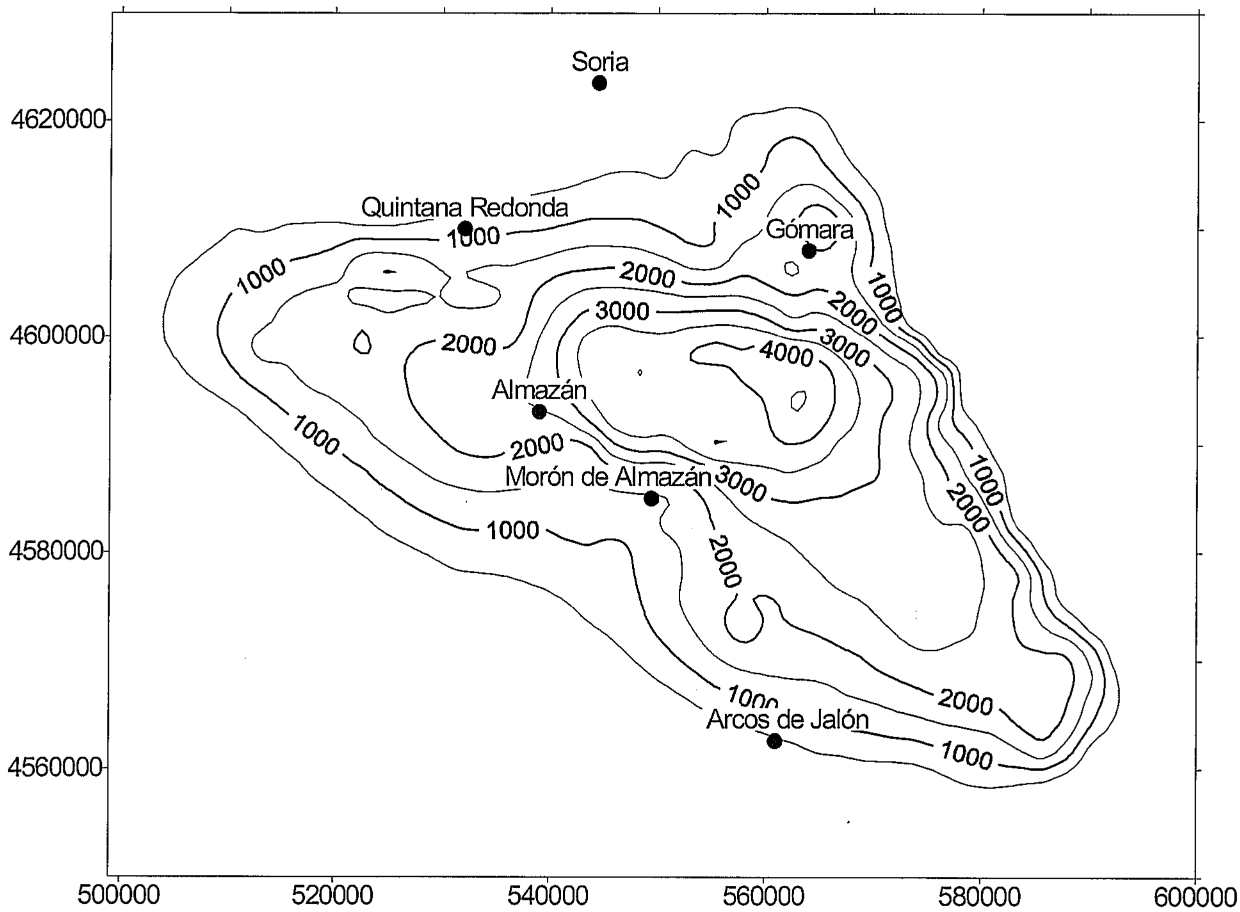


**Figure 2.-** Tertiary and Upper Cretaceous isopach map. Contour interval 500 m. UTM coordinates in metres, huse 30.

The aim of this paper is to investigate the crustal structure of the Almazán Basin by means of new gravity and previous seismic data. Oil research in this area provided reflection seismic profiles carried out by SHELL (1982). Migration and interpretation of these data reflects the basin geometry which allows us to determine the relationship between these data and the anomalies drawn in the gravity map which has been obtained from a gravity survey carried out for this purpose.

In order to analyse the different gravity sources causing the gravity anomalies, two methods have been applied. First, the gravity anomaly due to the Tertiary infill of the basin has been computed and removed. Second, to investigate the deep sources, a spectral analysis of the Anomaly Gravity map obtained by removing the basin gravity contribution has been carried out. All the above results together with the geological data have been integrated to establish three 2+1/2 D gravity profiles reflecting the basin and underlying basement structure.

## Methodology

The objectives previously proposed required the combination of several geophysical techniques aimed at obtaining a good knowledge of the basin and crustal structure for this area.

A brief discussion of the methodology is given below:

*Seismic data*

A total of 26 seismic profiles (SHELL, 1982) has been interpreted. For every seismic profile, the CDP (Common Depth Point) provides a single velocity data. Knowing the relationship between velocity and depth given by each CDP, the depth for a singular reflector along the seismic profiles can be deduced. The chosen reflector in all the profiles has been identified as the top Albian (Utrillas formation) in El Gredal well (SHELL, 1982). Density and distribution of seismic profiles are good enough to provide a detailed geometry for this reflector. After depth data obtained, a top Albian isopach map has been derived. Kriging with a regular grid of 2000 m resolution (Fig. 2) has been the interpolation method used. Maximum depth is located close to the easternmost boundary of the basin, reaching up to 4500 m in thickness, with an E-W trend. The calculated isopach map for this reflector shows slightly higher values than the previously one published by Bond (1996), but the geometry is similar.

*Theoretical gravity anomaly of the basin*

In some cases, where the geometry of a geological

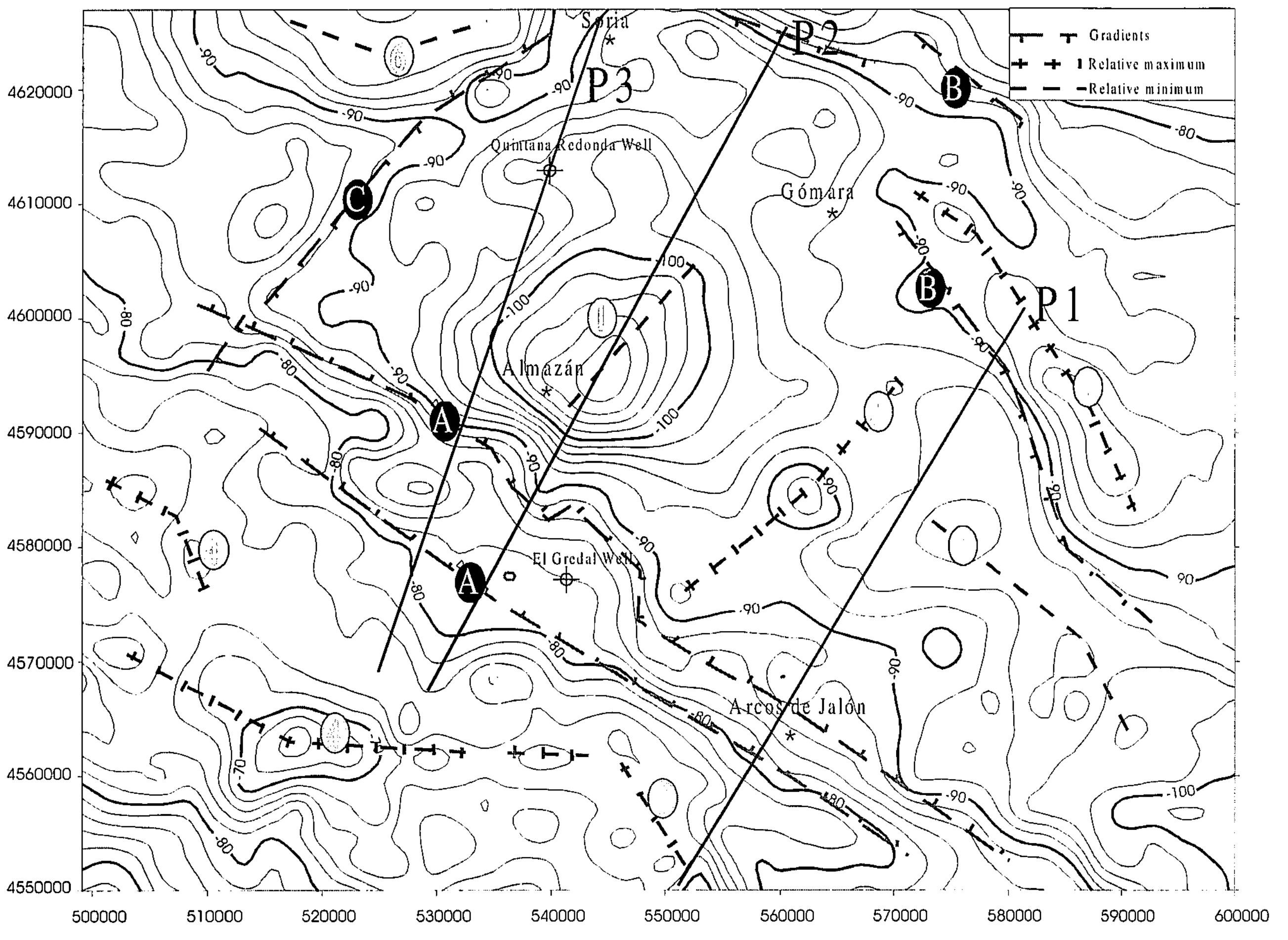


**Figure 3.**- Gravity anomaly map of the Almazán Basin. Contour interval 2 mGal. UTM coordinates as in figure 2. The location of the three gravity models is shown. Numbers and letters refer to features described on the text.

structure is well known from seismic and well data, it is useful to compute the gravity effect associated to that structure. The calculated effect can be removed from the observed gravity map, obtaining a new map that enhances the deep structure which effect was previously hidden by overlaying sediments. Gravity anomaly 3D computation results too complicated for most of the geological structures, being useful only for some relatively simple structures, such as sedimentary basins, diapiric structures or not very complex plutonic bodies (i.e. Yenes *et al.,* 1995). Different methods of 3D anomaly calculation are described in the literature (Cordell and Henderson, 1968; Chai and Hinze, 1988; Baskhara Rao *et al.*, 1990). It is commonly observed that sedimentary basin density increases with depth due to the high confining pressure in the lowermost zone. A method characterised by a density contrast varying with depth between model and host rock is used in this work. This density contrast is described by a quadratic function (Baskhara Rao, 1986).

3D gravity modelling of a sedimentary basin requires the construction of a regular grid whose spacing is determined according to the desired degree of accuracy, bearing in mind that computational time increases exponentially with grid side. In our case, a grid of 34 rows by 44 columns with a spacing of 2350 m has been chosen. Knowing the sedimentary thickness for every grid point, the sedimentary basin is represented by a group of juxtaposed prisms whose area is given by the square of the grid spacing, whereas its height is represented by the sedimentary thickness. From the expression for the gravity anomaly produced by a prism with variable density contrast (Bhaskara Rao *et al.*, 1990), the anomaly associated with every grid point is calculated by adding the gravity contribution of the prism located at this point and the effect of the surrounding prisms. This effect depends on the distance between every prism and the considered grid point. This algorithm has been used in the ANOMALIA computer program (Gómez D., unpublished), which provides a gravity map from an isopach map of the sedimentary basin and a quadratic function describing the relation between density contrast and depth.

The computed theoretical gravity map obtained for the sedimentary basin is subtracted from the observed gravity map in order to remove the gravity contribution of the sediments. As a result, the final map will be mainly affected by basement structures, lithological changes or structures whose gravity anomaly might be hidden by the effect of the sedimentary infill.

*Spectral analysis*

In order to obtain a good approach to the depth sources located under the sedimentary basin, a gravity spectral analysis based on a statistical method has been applied (Spector & Grant, 1970). One of the main problems in gravity analysis is the discrimination of the residual and regional sources because of the difficulty to discriminate long wavelengths due to superficial sources from those generated by sedimentary basins. To solve this problem, a spectral analysis from the basement structures map has been carried out. First, a 2D Fourier Analysis of the gravity map was worked out, using the technique described by Davis (1973). This method provides the amplitude for every harmonic component whose wavelength is a multiple of the fundamental wavelength, as defined by the length of the map. The amplitudes so obtained represent the frequency domain for the map. In this domain, the techniques of filtering and spectral analysis can be carried out more easily.

The square of the amplitudes for every harmonic component is called the power spectrum and represents the energy associated to every component. A graphic representing the power spectrum versus the radial frequency provides an estimation of the mean depth around which the sources are distributed. In most cases, three linear segments can be distinguished. Each linear segment corresponds to a different source and is characterised by a frequency interval and a slope, which is directly related to the mean depth of the source. In our case, regional and residual sources have been isolated by means of a Wiener filter (Gupta & Ramani, 1980).

*Gravity modelling*

Depths derived from seismic and geological data, as well as rock densities obtained from rock samples and density log data have been integrated in a density model which has been used for the modelling, together with the spectral analysis results.

Modelling has been carried out with a GM-SYS software, which uses the algorithm described by Won & Bevis (1987). This is a straightforward method, which by means of trial and error and varying the body geometry allows to obtain a good fitting between theoretical and observed anomalies. This fitting must be under an error value considered as acceptable in function of the error map, gravity station spacing and the regional or more detailed character of the study.

## Gravity Anomaly map

In order to achieve the aforementioned goals, a gravity survey of the Almazán Basin and the surrounding areas has been carried out. A total of 907 gravity stations homogeneously distributed in an area of 8000 km$^2$ has been obtained, providing a 0.11 stations/km$^2$ density. The gravity meter used in the survey has been the Lacoste & Romberg model G, number 953 with a theoretical accuracy of ± 0.01 mGal and drifts lesser than ± 1 mGal per month. The height for each station has been determined using a barometric altimeter (Pauling model MD-5) with an accuracy of ±1 m. The density reduction chosen for this study has been 2.67 gr/cm$^3$. Terrain correction has been computed up to 22 km; the first 170 m were calculated in the field, and the rest calculated from a Digital Elevation Model (DEM) (Kane, 1962). This DEM has been constructed digitising 1:50.000 scale topographic maps.

Using the kriging method, a gravity map of 34 rows by 44 columns with a 2325 m spacing grid has been drawn (Fig. 3). The length of the map is 100 km in the E-W direction and 80 km in the N-S direction. The mean square error of the map is ±1.69 mGal.

The gravity map is characterised by several relative-gravity highs and lows, as well as strong gradients. The regional features of the map are a relative low with NW-SE trend, corresponding to the Almazán Basin, and two relatives highs associated to the Aragonian and Castillian branches of the Iberian Range. Three different structures can be distinguished inside the basin: a relative low (Almazán low), with a NNE-SSW mean trend (1), a relative high (2) trending parallel to the previous low, and a relative low (3) trending NW-SE and located close to the south-eastern basin boundary. The gravity low located at Almazán (1) is linked to a basin depocenter, but there is no clear correspondence between the isopachs map and gravity for the rest of the sedimentary basin. The gravity low related to the basin is bounded to the south by a gradient trending N110° E (A), which shows a maximum associated (4) to the Castillian branch of the Iberian Range; this gradient is linked to re-activated late Variscan faults affecting the southwestern basin boundary (Bergamín *et al.*, 1995; Bond, 1996). The limit between the Almazán Basin and the Aragonian branch of the Iberian Range (5) is drawn by NW-SE trending gradient (B) associated to the basin marginal structure. The northwestern boundary of the Almazán Basin is constituted by a NE-SW trending gradient (C) associated to the Soria Fault (Maestro *et al.*, 1994). This corresponds to the south-eastern boundary of Cameros Basin that extends towards the Almazán basin-Duero Basin linking area. The Cameros basin is depicted by a relative gravity low (6).

## Theoretical gravity map and spectral analysis of the basin

The theoretical gravity map (Fig 4) of the sedimentary infill has been calculated from the isopach map by means of the computer program ANOMALIA with the method described above. Density contrast has been obtained by least squares fit, using a quadratic function of the density data obtained from El Gredal well (SHELL, 1982) (Fig. 5). The density function varies from 2.46 gr/cm$^3$ to 2.69 gr/cm$^3$. The maximum anomaly value obtained is –16 mGal.

Figure 6 shows the resulting map after removing the

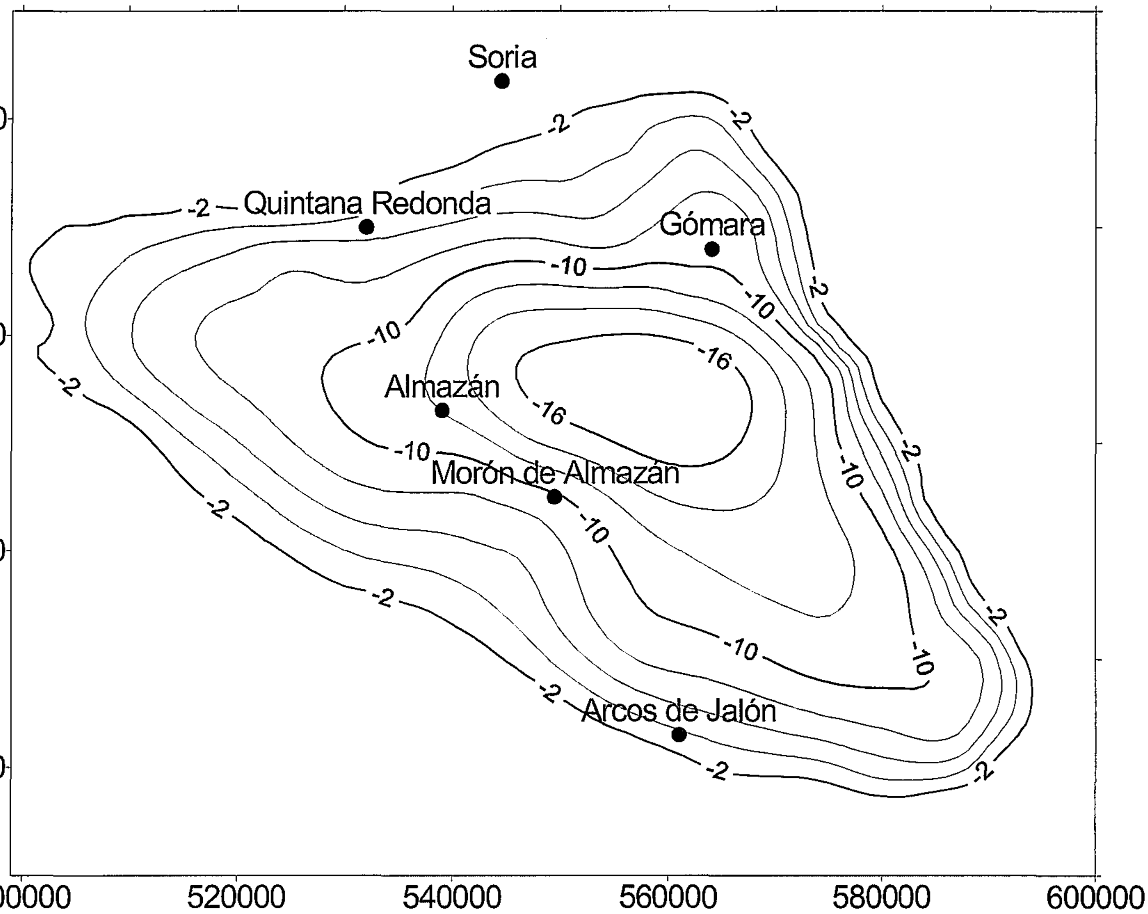


**Figure 4.-** Theoretical gravity anomaly map, showing the gravity effect of the sedimentary infill, using a density ranging at depth from 2.46 gr/cc to 2.69 gr/cc. Interval 2 mGal. UTM coordinates as in figure 2.

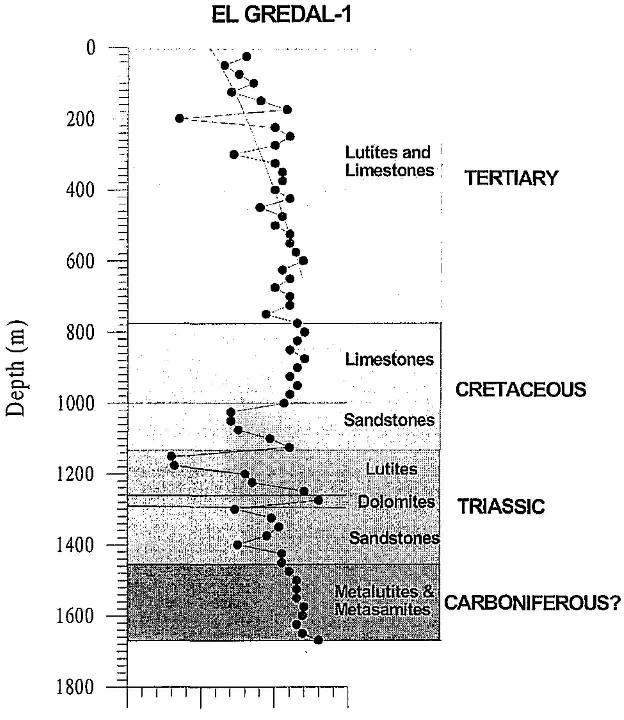


**Figure 5.-** Density log derived from El Gredal well. See location on figure 3. Black line between 0 and 700 m depth represents the least square fit to a quadratic function for depth variation density. The density obtained has been used for the computation of the gravity anomaly depicted on figure 4.

gravity effect of the basin from the observed gravity map. The Almazán gravity low has been widely attenuated in this map and the gravity high located between Gómara and Arcos de Jalón has been increased reaching values up to –74 mGal. We interpret that this map reveals the occurrence of bodies with different densities in the basement.

In order to establish the depth to the sources located under the sedimentary basin more accurately, a spectral analysis of gravity data based on a statistical method has been applied (Spector & Grant, 1970). A graphic representing power spectrum versus radial frequency provides an estimation of the mean depth around which the sources are distributed. In most of the cases (Syberg, 1972; Gupta & Ramani, 1980; Pawlowski, 1994), three linear segments can be distinguished. Each linear segment corresponds to a different source and is characterised by a frequency interval and a slope, which is directly related to the mean depth of the source. Applying this method to our gravity map, three sources can be distinguished (Fig. 7). The first one corresponds to a radial frequency lower than 0.2 $km^{-1}$ (wavelength greater than 31 km) and its estimated depth is 11 km ± 0.55. This is the deepest source obtained for this work and will be called the regional source. Because of its depth and wavelength, this source seems to be associated to the limit between the middle crust and the base-

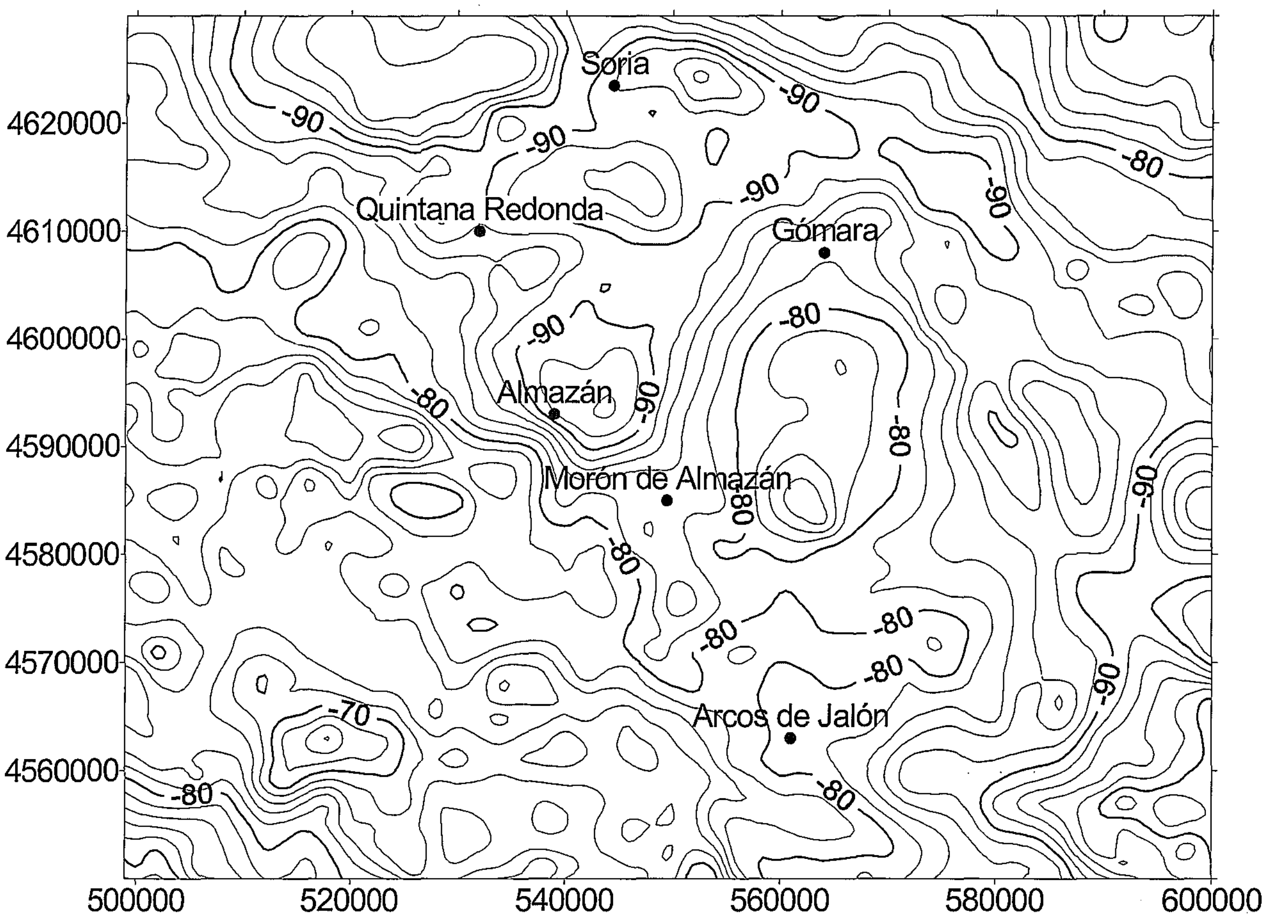


**Figure 6.-** Theoretical gravity anomaly map obtained by subtracting the gravity anomaly map due to the sedimentary infill from the observed gravity anomaly map. Contour interval 2mGal. UTM coordinates as in figure 2.

ment (or upper crust) in good coincidence with the data presented by other authors (Guimerà & Alvaro, 1990). A linear segment corresponding to the frequency interval 0.2-0.8 $km^{-1}$ (wavelength ranging from 31 and 7.8 km) defines the second source, whose calculated depth is 4.4 km ±0.19. This source displays an unclear significance, and it could be due to changes in the basement density, as previously described in some neighbouring areas (Rivero *et al.*, 1996) or to irregularities in the basement-cover limit in the deepest part of the Almazán Basin. The third linear segment, with a gentle slope and defined by frequencies greater than 0.8 $km^{-1}$ is related to white noise. White noise corresponds to the high-frequency noise due to the acquisition and processing of geophysical data, rounding errors in spectral analysis, etc.., and so will not be considered in the modelling process.

As a result of the data derived from the spectral analysis of the gravity map without the contribution of the basin infill, a Wiener type filter has been designed (Gupta & Ramani, 1980). As mentioned before the parameters of the filter are derived from the frequencies and depths obtained for every source. Applying the filter to the gravity map, a new Bouguer anomaly map (Fig. 8) has been drawn, showing the effect of the regional source alone. The anomaly ranges from –68 mGal

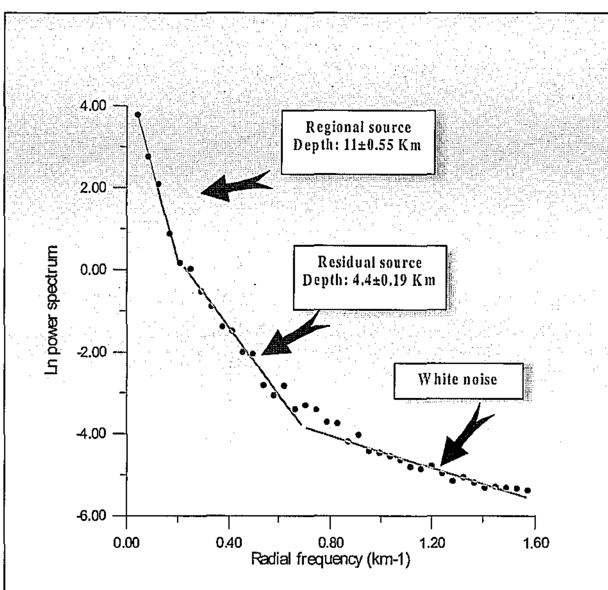


**Figure 7.-** Graph showing power spectrum versus radial frequency for the gravity map in figure 3. Three different sources, regional, residual and white noise are distinguished, and their mean depths have been calculated.

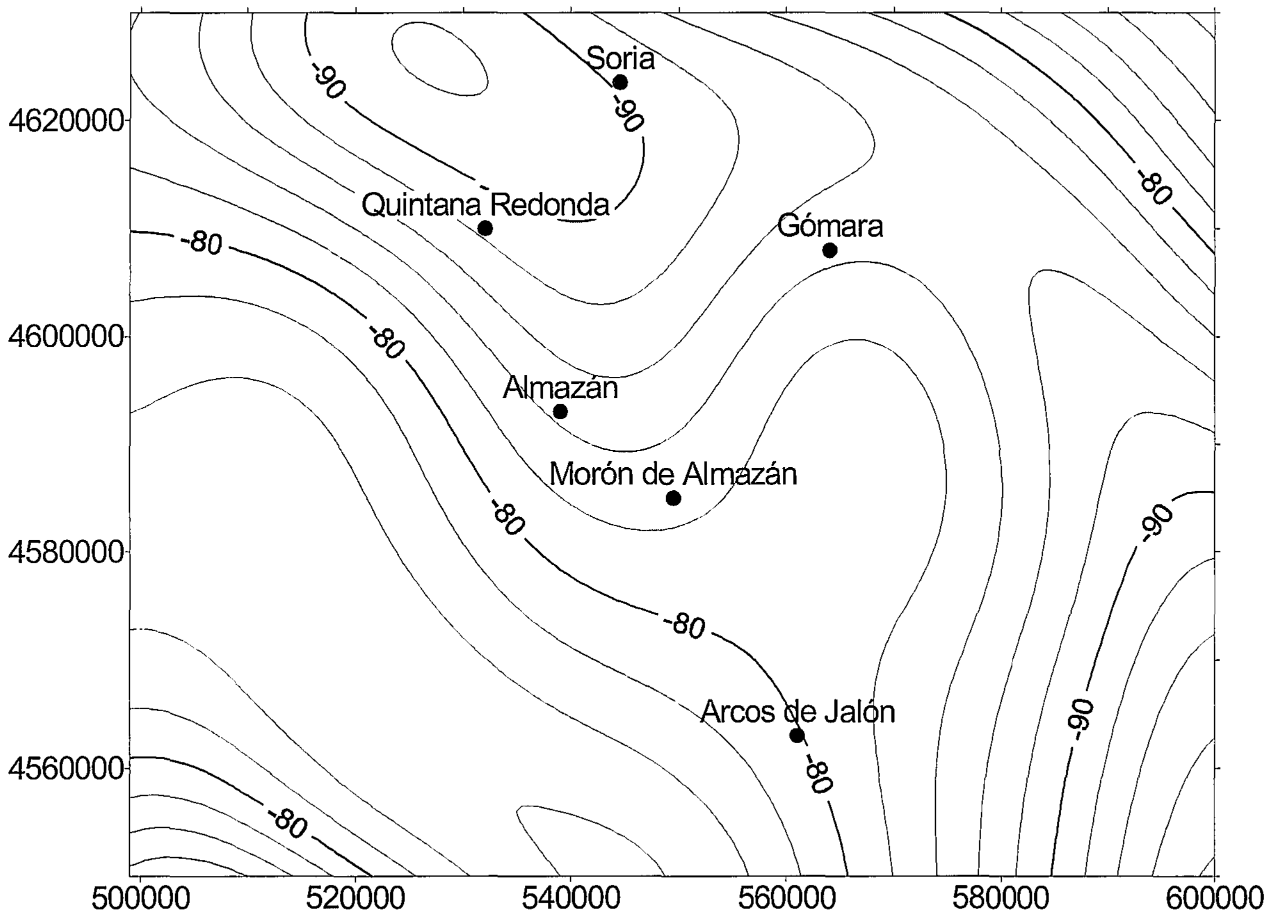


**Figure 8.-** Bouguer anomaly map showing the effect of the regional source isolated. Contour interval 2 mGal. UTM coordinates as in figure 2.

to –101 mGal. This map shows a minimum trending NW-SE with a superimposed maximum with a NE-SW orientation.

## Gravity modelling

Three 2+1/2 D gravity models trending NE-SW have been performed (Fig. 9). The model length of the models ranges from 80 km to 90 km. The information provided by seismic profiles and surface geology has been used to model the shallower structures and the basin geometry. Density data come from the density log of El Gredal well and rock samples collected in the whole studied area. The integration of deep structure, derived from spectral analysis, and surface geology provides gravity models which satisfactorily fit the observed anomaly.

*Profile 1*

The gravity profile 1 is located at the easternmost part of the basin (Fig. 3), extending from the Castillian branch of the Iberian Range to the Aragonian branch. The observed anomaly ranges from –69 mGal to –95 mGal. The initial geological model has been established on the basis of geological mapping data (Adell Argiles, 1982; Ferreiro, 1991; Lendínez, 1991a, b, c; Lendínez & Martín, 1991; Lendínez & Ruiz, 1991) and a seismic line (A8011, SHELL 1982). A satisfactory fit can be reached with eight different bodies. Two bodies whose age is Miocene and Palaeogene represent the sedimentary infill. Their densities are 2.49 gr/cm$^3$ and 2.51 gr/cm$^3$ respectively. The Palaeogene unit reaches a maximum thickness of about 2000 m whereas the Miocene unit reaches 500 m.

An Upper Cretaceous unit with a thickness of 200 m and a density of 2.66 gr/cm$^3$ is present in the whole basin defining its base. The basin seems to draw a flat geometry in this area, but in its northeastern limit, it appears folded and affected by a reverse fault, which constitutes the boundary of the basin with the Aragonian branch of the Iberian Range.

Two bodies with densities 2.64 gr/cm$^3$ and 2.65 gr/cm$^3$ represent the Jurassic and Triassic units respectively. They lie under the Cretaceous unit, but only to the southwestern part of the model. This is probably due to the fact that this formed a paleogeographical high during Mesozoic times, which was later eroded in the Upper Cretaceous.

Bearing in mind the regional source map trend, the Middle-Upper crust limit has to be shifted from a depth of 9 km in the SW to 13 km in the NE, in order to obtain a good fit. Nevertheless, it has been necessary to introduce two different Upper crust basements with densities 2.68 gr/cm$^3$ and 2.70 gr/cm$^3$, whose contact seems to be a discontinuity dipping SW. This discontinuity is coincident with the trend and vergence of the Variscan

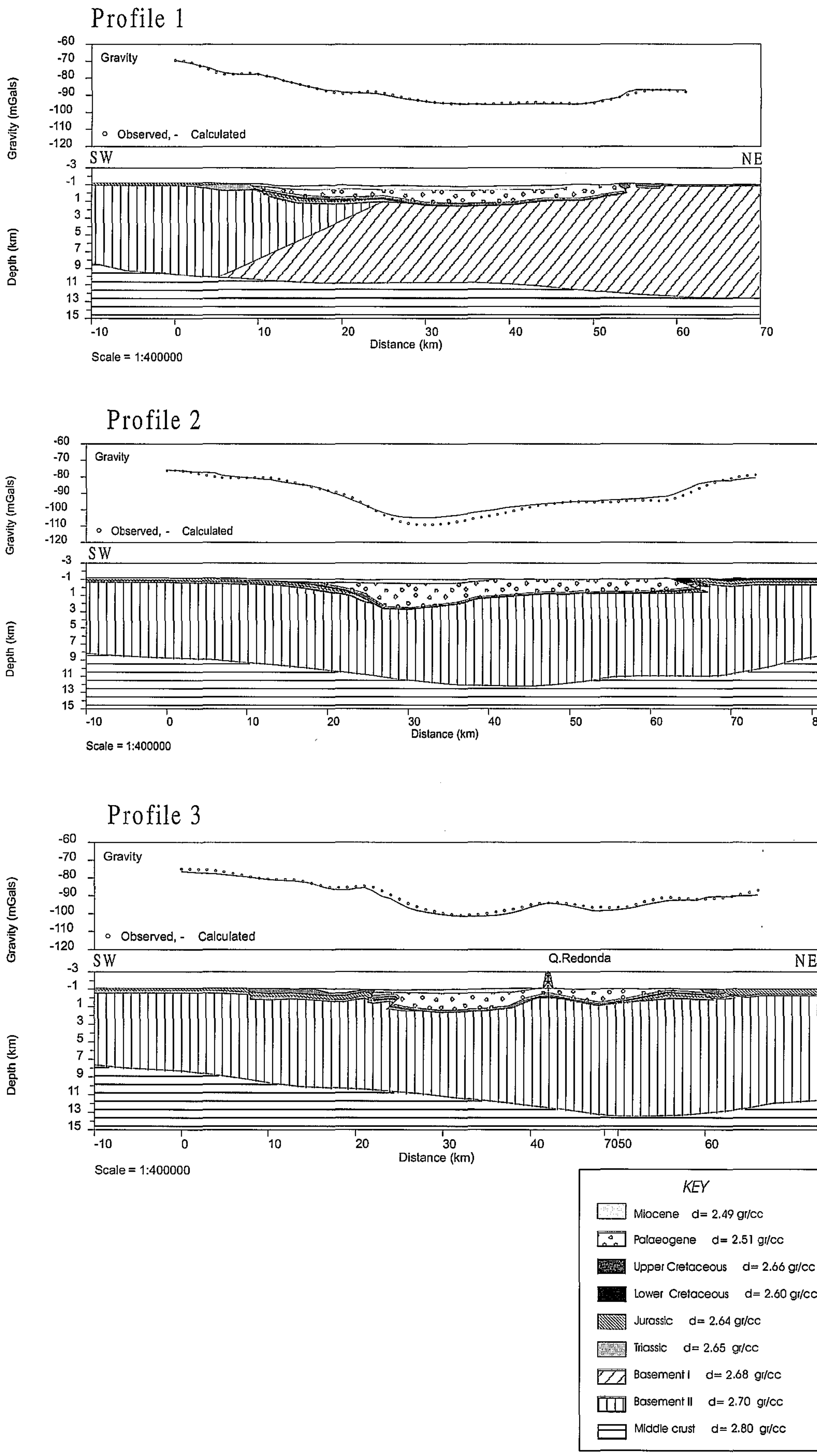


**Figure 9.-** 2+1/2 D gravity models representing the boundary between basement and middle crust as well as surface geology and basin geometry as deduced from seismic data. No vertical exaggeration.

structures observed in the Palaeozoic outcrops in the Aragonian branch of the Iberian Range.

The deepest body represents the Middle crust (2.80 gr/cm$^3$). Its density has been chosen on the basis of previous works developed in surrounding areas, and it has been determined from seismic refraction data (Tejero *et al.*, 1996). The top of this body shows an staircase geometry, increasing its depth from 9 km in the southwestern border to 11 km beneath the basin, reaching 13 km in the northeastern limit. A gentle uplift coincident with the gravity high is better observed when the basin gravity contribution was removed.

*Profile 2*

This profile is sited in the central part of the basin (Fig. 3). Its trend is similar to that of the profile 1, and the geological constraints are also geological mapping and the A8014 seismic profile. This model goes through the depocenter as obtained from the seismic interpretation, reaching a sedimentary thickness of 3500 m. Its anomalies vary from −76 mGal to −109 mGal.

In this model a new unit is defined corresponding to the Lower Cretaceous (Weald facies) with a density of 2.60 gr/cm$^3$. Densities for the other units are the same than for profile 1. The Miocene unit shows a similar thickness, but the Palaeogene unit reaches up to 3000 m, coincident with the minimum of −110 mGal observed in the gravity map.

As in the previous model, the Upper Cretaceous body defines the bottom of the basin but it is not present in the southwestern border, probably because it was eroded by the Miocene unit.

Both the Triassic and Jurassic units are discontinuous beneath the whole basin, and they disappear in the central part (ITGE, 1990). No major faults are involved in the southwestern border of the basin, whereas several reverse faults are observed in its northeastern limit, where lower Cretaceous units overlay upper Cretaceous and Palaeogene units.

In the basement, it is only necessary to introduce a body with a density of 2.70 gr/cm$^3$. Taking into account the regional trend and the depth discontinuity obtained from the spectral analysis of the regional source, the boundary between the Upper and Middle crust shows a depression of about 3 km. This limit is located at 9 km depth in the southwestern edge and reaches 12 km depth beneath the basin, although the maximum depth is shifted towards the northeast in relation to the basin depocenter. A slight misfit between the observed and calculated anomaly can be observed in this profile, located at the maximum Tertiary sedimentary thickness. As there is an acceptable fit in profiles 1 and 3 using the densities obtained from El Gredal well (where basin depth is lower than in profile 2), this misfit could be due to a density decrease in the inner part of the basin.

*Profile 3*

This profile is the westernmost one (Fig. 3) and is also coincident with a seismic line (A 8054D; SHELL, 1982). The observed anomaly varies from −74 mGal to −101 mGal. In this case, subsurface data from the Quintana Redonda well have been incorporated.

The Miocene and Palaeogene units show the same characteristics as in profile 2, but the maximum Palaeogene thickness is only 2000 m. A minor depocenter is located towards the northeast, where it reaches up to 1500 m in depth. The Cretaceous unit is present in the whole basin, increasing its thickness towards both edges of the model. The lack of Triassic and Jurassic units is a characteristic already described in profiles 1 and 2. The structure in the northeaster border of the basin is, again, constituted by reverse faults dipping NE. A new fact revealed in this model is the occurrence of two major reverse faults affecting all Mesozoic units; the northeasternmost fault throws up about 1500 m. These faults were eroded by Miocene sediments and do not reach the surface. Two major anticlines related to the previous faults can also be observed.

As in profile 2, only a body with a 2.70 gr/cm$^3$ density is present in the basement. As in the previous profiles, considering the regional source trend, Upper-Middle crust boundary shows a depression located at the northeastern part of the basin. This boundary locates 13 km down in the most depressed area, starting with a 9 km depth in the southeastern limit.

## Conclusions

The geometry of the Almazán Basin has been established by combining gravity data, seismic data and modelling. According to the interpretation of seismic reflection profiles, the maximum Tertiary sedimentary thickness is located along an approximately E-W trending depocenter, spreading from the town of Almazán towards the Aragonian branch of the Iberian Range. Maximum depth reaches more than 4000 m below present topography.

The Bouguer Anomaly map shows that only the westernmost part of the isopach map is related to the major gravity low located at the central part of the basin, whereas the easternmost part does not show a clear relationship between sedimentary thickness and the gravity map.

By computing the theoretical gravity effect of the sedimentary infill and removing it from the observed gravity map, a relative gravity high (with a NE-SW trend) has been enhanced (Fig. 6). The source causing this anomaly is located beneath the basin.

The spectral analysis carried out on the theoretical gravity anomaly map (subtracting the sedimentary infill gravity effect) has revealed two discontinuities located at 4.4 and 11 km depth.

Integrating all the aforementioned results, three gravity profiles have been obtained. The analysis of these profiles provides the following common features:

a) The basement thickens northeastwards near the Cameros Basin and the Arangonian Branch of the Iberian Range.

b) Basin depth, as obtained from seismic profiles interpretation, seems to fit well the gravity models.

c) Density log from El Gredal well has provided density values that are in good agreement with the modelling of the gravity response of the sedimentary infill.

d) As deduced from the three gravity profiles, the northeastern border is depicted as a fault, where Mesozoic sediments overlie the Tertiary basin.

e) To achieve a good fit in profile 2, it has been necessary to introduce two bodies with different densities in the basement.

In order to confirm the occurrence of these structures, more gravity models are necessary. The ambiguity inherent to the modelling process using these geophysical data separately could be reduced by combining seismic and gravity data together with spectral analysis techniques.

We wish to thank the reviewers Dr. Gabriel Gutiérrez Alonso and Dr. J. Aller helped greatly to clarify the final version of the manuscript. This study was supported by the DGICYT of Spain, project PB98-0846.

## References

Adell Argiles, F. (1982): Mapa Geológico de España a escala 1:50.000. Hoja nº 434, Barahona. IGME. 56 p. and one map.

Armenteros, I., Dabrio, C. J., Guisado, R. & Sánchez de Vega, A. (1989): Megasecuencias sedimentarias del terciario del borde oriental de la Cuenca de Almazán (Soria-Zaragoza). *Stvdia Geológica Salmanticensia*, Vol. Esp. 5: 107-127.

Bergamín J.F., Tejero, R. & Pinto, V. (1995): Modelización gravimétrica en 2 ½ D y 3 D en la zona nororiental de la Cuenca de Madrid. *Rev. Soc. Geol. España*, 8 (3): 251-259.

Bhaskara Rao, D. (1986): Modelling of sedimentary basins from gravity anomalies with variable density contrast. *Geophy. Jour. Roy. Astr. Soc.*, 84 (1) : 207-212.

Bhaskara Rao, D., Prakash, M.J. & Ramesh Babu, N. (1990) : 3D and 2 ½ D modelling of gravity anomalies with variable density contrast. *Geophy. Prosp.*, 38 (4) : 411-422.

Bond, J. (1996): Tectono-sedimentary evolution of the Almazán Basin, NE Spain. In: *Tertiary basins of Spain: the stratigraphic record of crustal kinematics* (Friend, F. and Dabrio, C.J., Eds). Cambridge University Press: 203-213.

Casas, A.M., Cortés, A.L. & Maestro, A. (in press): Intra-plate deformation and basin formation during the Tertiary at the northern Iberian plate: Origin and evolution of the Almazán basin. *Tectonics.*

Chai Y. & Hinze W. J. (1988) : Gravity inversion of an interface above which the density contrast varies exponentially with depth. *Geophysics*, 53 (6): 837-845.

Clemente, P. & Pérez Arlucea, M. (1993): Depositional architecture of the Cuerda del Pozo Formation, lower Cretaceous of the extensional Cameros Basin, North-Central Spain. *Jour. Sediment. Petrol.*, 63: 437-452.

Cordell, L. & Henderson, R.G. (1968): Iterative three-dimensional solution of gravity anomaly data using a digital computer. *Geophysics*, 33 (4): 596-601.

Davis, J.C. (1973): *Statistics and data analysis in geology.* John Wiley and Sons, New York, 550 p.

Ferreiro, E. (1991a): Mapa Geológico de España a escala 1:50.000. Hoja nº 377, Burgo de Osma. ITGE. 39 p. and one map.

García-Hidalgo, J.F., Segura, M. & García, A. (1997): El Cretácico del borde septentrional de la Rama Castellana de la Cordillera Ibérica. *Rev. Soc. Geol. España*, 10 (1-2): 39-54.

Gómez Ortíz, D. (1997): ANOMALÍA. Programa para el cálculo de la anomalía de Bouguer generada por una cuenca sedimentaria (Unpublished).

Goy, A., Gómez, J.J. & Yébenes, A. (1976): El Jurásico de la Rama Castellana de la Cordillera Ibérica (mitad norte). I. Unidades litoestratigráficas. *Estudios Geol.*, 32: 391-423.

Goy, A. & Suárez Vega, L.C. (1983): Tectónica y estratigrafía mesozoicas: El Jurásico. In: *Geología de España. Libro Jubilar J.M. Ríos*, (J.A. Comba, Coord.) Vol. II, Instituto Geológico y Minero de España, 62-79.

Guimerà, J. & Alvaro, M. (1990): Structure et evolution de la compression alpine dans la Chaîne Ibérique et la Chaîne Cotiére Catalane (Espagne). *Bull. Soc. Geol. France,* 8ème série, VI: 339-340.

Guimerà, J., Alonso, A. & Mas, J.R. (1995): Inversion of an extensional-ramp by a neoformed thrust: the Cameros Basin (N Spain). In: *Basin Inversion* (J. G. Buchanan and P. G. Buchanan, Eds.), *Geol. Soc.* Spec. Publ. 88, 443-453.

Gupta, V.K. & Ramani, N. (1980) : Some aspects of regional-residual separation of gravity anomalies in a Precambrian terrain. *Geophysics*, 45 (9) : 1412-1426.

I.T.G.E (ed.) (1990): *Documentos sobre la geología del subsuelo de España, Vol. 5: Duero-Almazán.* Instituto Tecnológico Geominero de España, Madrid, 20 maps.

Kane, M. F. (1962): A comprehensive system of terrain corrections using a digital computer. *Geophysics*, 27 (4): 455-462.

Lendínez, A. (1991a): Mapa Geológico de España a escala 1:50.000. Hoja nº 350, Soria. ITGE. 239 p. and one map.

Lendínez, A. (1991b): Mapa Geológico de España a escala 1:50.000. Hoja nº 380, Borobia. ITGE. 96 p. and one map.

Lendínez, A. (1991c): Mapa Geológico de España a escala 1:50.000. Hoja nº 435, Arcos de Jalón. ITGE. 62 p. and one map.

Lendínez, A. & Martín, D. (1991): Mapa Geológico de España a escala 1:50.000. Hoja nº 436, Alhama de Aragón. ITGE. 68 p. and one map.

Lendínez, A. & Ruiz, V. (1991): Mapa Geológico de España a escala 1:50.000. Hoja nº 408, Torrijo de la Cañada. ITGE. 90 p. and one map.

Maestro, A., Casas, A.M. & Cortés, A.L. (1994): El campo de esfuerzos terciarios en la Cuenca de Almazán (provincias de Soria y Zaragoza). *II Congreso de G.E.T.*, Jaca: 149-152.

Parker, R. L. (1972) : The rapid calculation of potential anomalies. *Geophys. J. R. astr. Soc.*, 31 : 447-455.

Pawlowski, R. S. (1994): "Green's equivalent-layer concept in gravity band-pass filter design". *Geophysics*, 59(1): 69-76.

Platt, N.H. (1990): Basin evolution and fault reactivation in the Western Cameros Basin, Northern Spain. *Jour. Geol. Soc. London*, 147: 165-175.

Rey Moral, C., Tejero, R. & Gómez Ortiz, D. (1998): Estudio de la estructura de la Cuenca de Almazán a partir de datos geofísicos. *Geogaceta,* 24: 259-262.

Rivero, L., Guimerà, J. & Casas, A. (1996) : Estructura profunda de la Cuenca de Cameros (Cordillera Ibérica) a partir de datos gravimétricos. *Geogaceta*, 20 (7) : 1695-1697.

Sanz de Galdeano, C.M. (1996): Tertiary tectonic framework of the Iberian Peninsula. In: *Tertiary basins of Spain: the stratigraphic record of crustal kinematics* (P.F. Friend and

C.J. Dabrio, Eds.). Cambridge University Press: 9-14.
SHELL (1982): *Informe final del sondeo El Gredal-1*. Permiso Exploración de Almazán Shell España, N.V.
Spector, A. & Grant, F. S. (1970): Statistical methods for interpreting aeromagnetic data. *Geophysics*, 35 : 293-302.
Syberg, F. J. R. (1972): A Fourier method for the regional-residual problem of potential fields. *Geophysical Prospecting*, 20: 47-75.
Tejero, R., Perucha, M. A. & Bergamín, J. F. (1996): Modelos gravimétrico y estructural del Sistema Central. *Geogaceta*, 20 (4): 947-950.
Won, I.J. & Bevis, M. (1987): Computing the gravitational and magnetic anomalies due to a polygon: Algorithms and Fortran subroutines. *Geophysics*, 52: 232-238.
Yenes, M., Gutiérrez-Alonso, G., Álvarez, F., Díez-Balda, M. A.. & Vigneresse, J. L. (1995): Aproximación a un modelo gravimétrico en tres dimensiones (3D) de los granitoides del área de La Alberca-Béjar (Zona Centro-Ibérica). *Rev. Soc. Geol. España*, 8 (1-2): 51-59.

*Manuscript received 20 December 1999*
*Accepted 23 May 2000*